THE ASTROPHYSICAL JOURNAL, 455:456–467, 1995 December 20

THE SOFTEST X-RAY SOURCES IN THE *ROSAT* POINTED CATALOG: WGACAT

K. P. SINGH,[1,2,3] P. BARRETT,[1,4,5] N. E. WHITE,[1,6] P. GIOMMI,[7,8] AND L. ANGELINI[1,4,9]

Received 1995 April 19; accepted 1995 June 30

ABSTRACT

We present a selection of X-ray sources with the softest observed spectral characteristics and discuss their nature. These "ultrasoft" sources were detected in 3 years of pointings with the *ROSAT*. These sources are predominantly found to be white dwarfs, magnetic cataclysmic variables, nearby late-type stars, and very X-ray soft active galactic nuclei. The broadband colors of the unidentified ultrasoft sources suggest that a number of them may have at least two components in their spectrum, as for example, is found in most cataclysmic variables. Some of these objects may represent the extreme of their respective populations, for example, unusual galaxies, "supersoft" sources with steep low-energy spectrum and high X-ray luminosity ($\sim 10^{38}$ ergs s^{-1}), active galactic nuclei, stars, etc. Follow-up studies in the optical and other wavebands are needed.

Subject headings: galaxies: active — novae, cataclysmic variables — white dwarfs — X-rays

1. INTRODUCTION

The recent availability of the soft X-ray source catalog of 62,000 sources by White, Giommi, & Angelini (1994, henceforth WGACAT), constructed from 3 years of *ROSAT* pointings is a very valuable resource for identifying and studying many different classes of X-ray emitters. For example, a new class of "supersoft" X-ray sources, characterized by a blackbody spectrum with a temperature of a roughly a few times 10 eV and a bolometric luminosity of $\sim 10^{38}$ ergs s^{-1}, has recently been discovered with *ROSAT* (Hasinger 1994). Although first discovered in the Magellanic Clouds, examples of supersoft sources have also been found in our Galaxy (Beuermann et al. 1995), and in the M31 galaxy (White et al. 1995). In addition to this new type of supersoft sources, believed to be accreting white dwarfs (van den Heuval et al. 1992), there are other classes of objects which have extremely soft X-ray spectra. The most prominent of these are white dwarfs (WDs) (see Barstow et al. 1993), magnetic cataclysmic variables (MCVs, magnetic field $B \geq 100$ kG), and some late-type stars. We have attempted to isolate the softest X-ray sources listed in the latest version (Rev. 1.0) of the WGACAT. These detections have spectral properties similar to that of WDs, MCVs, late-type stars, and some active galactic nuclei (AGNs). Therefore, we believe that we have identified many new MCVs, WDs, and other assorted classes of objects worthy of follow-up observations at other wavelengths.

2. *ROSAT* PSPC: SOFTNESS AND HARDNESS RATIOS

WGACAT is based on observations with the *ROSAT* X-ray telescope and a position sensitive proportional counter (PSPC) as the detector (Trümper 1983; Pfeffermann et al. 1987). The PSPC has an energy resolution ($\Delta E/E$) of $\simeq 0.42$ at 1 keV and a bandwidth of 0.1–2.4 keV. The energy of X-rays is analyzed using a pulse height analyzer (PHA) with 256 channels. The source counts for WGACAT are calculated for three broad bands of PHA channels: low band for PHA channels 11–39 corresponding to energy range of 0.1–0.4 keV, midband for PHA channels 40–85 corresponding to energy range of 0.4–0.9 keV, and a high band for PHA channels 86–200 corresponding to energy range 0.9–2.0 keV. The softness and hardness ratios (henceforth SRs and HRs, respectively) of the sources are then defined as the ratio of low band to midband counts, and the ratio of high band to midband counts, respectively.

3. DISTRIBUTIONS OF SOFTNESS RATIO

We examined the softness ratio distribution for the WGACAT sources identified with the most commonly known classes of sources, viz., AGNs, stars, and galaxies from several catalogs (White et al. 1994; for details, please refer to the *ROSAT* home page on the World Wide Web at the address given in the reference section). For this purpose we selected all available entries of identified sources with a signal-to-noise ratio of ≥ 3.0, and SR $\geq 2\sigma_{SR}$ where σ_{SR} is the 1 σ in SRs. All observations of a particular source were accepted, so that effects of variability are included in the analysis. The histograms of SRs for different classes are shown in Figures 1*a* and 1*b*. Figure 1*a* is based on 4414 observations of late-type stars, and 1137 observations of early-type stars, Figure 1*b* is based on 1854 observations of AGNs, and 2625 observations of galaxies. The distribution of SRs for AGNs and late-type stars seems to level off around a median value of 2, whereas that for galaxies and early-type stars continues to rise. All the distributions in Figures 1*a* and 1*b* drop sharply near 10, signifying the difficulty of detecting very soft objects or their lack thereof among the commonly known populations of sources. Very few or a negligible fraction of AGNs, galaxies, and early-type stars have SRs greater than 10. Some late-type stars, however, do have SRs greater than 10 and for some of them the SRs even extend beyond the referenced limit of 14.5 in the Figures 1*a* and 1*b*. The distributions shown in Figures 1*a* and 1*b* can be compared with the histogram of SRs shown in Figure 2 for a sample of $\simeq 15{,}000$ well defined sources detected in the

[1] Code 668, Laboratory for High Energy Astrophysics, NASA/GSFC, Greenbelt, MD 20771.
[2] NRC-NASA Senior Research Associate, on leave from Tata Institute of Fundamental Research, Bombay, India.
[3] kps@rosserv.gsfc.nasa.gov.
[4] Universities Space Research Association.
[5] barrett@piglet.gsfc.nasa.gov.
[6] white@adhoc.gsfc.nasa.gov.
[7] European Space Information System, Information Systems Division of ESA, ESRIN, via Galileo, 00044 Frascati, Italy.
[8] giommi@mail.esrin.esa.it.
[9] angelini@lheavx.gsfc.nasa.gov.

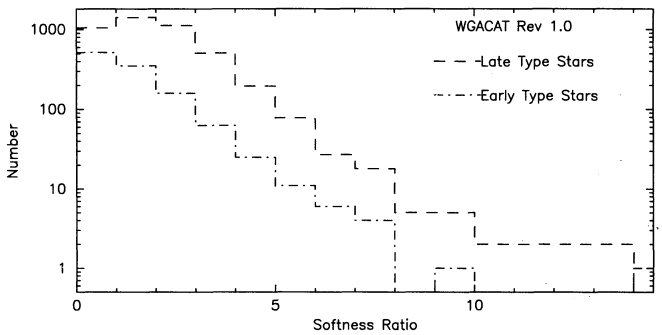

FIG. 1*a*

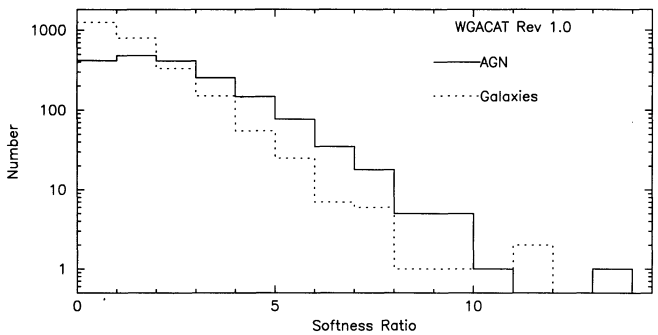

FIG. 1*b*

FIG. 1.—Histogram of softness ratio for observations of sources identified with (*a*) late-type stars and early-type stars, (*b*) AGNs and galaxies, in the WGACAT

WGACAT, and which remain unidentified in the catalog. The comparison shows that the distribution in Figure 2 is much broader than in Figure 1 and that there is a significant number of unidentified objects with SRs ≥ 8, the tail end of the distribution in Figure 1. To examine what kind of objects are likely to have such large values of SRs, we looked at other classes of objects and found that those classified as WDs (McCook & Sion 1987), and CVs (Shara, Shara, & McLean 1993) are the most likely ones to have large values of SRs. A histogram of SRs for WDs and CVs is shown in Figure 3, which shows a broad distribution for WDs in the range 0–20 and a secondary peak near 100. The distribution of CVs, however, is almost similar to that of other objects in Figure 1, with the exception of a possible secondary peak in the range 20–40 for the CVs. The identification of CVs in the WGACAT is based mostly on the catalog by Shara et al. (1993), and a number of recently discovered CVs have been missed (see below). Based on the data in Figures 1 and 3, we have quantified the frequency of occurrence of broad categories of identified objects in a histogram in Figure 4, which displays the percentage distribution of SRs for (1) late and early-type stars, (2) galaxies and AGNs, and (3) CVs and WDs. The different classes in Figures 1 and 3 were merged for convenience of representation. This diagram shows that the frequency of occurrence with SRs ≥ 10 is highest for CVs and WDs. Although a few stars may also have high values of SRs, it is possible that some of these objects may be misclassified. Based on the distributions shown in Figures 1–4, we assign the name of Ultrasoft Sources (to distinguish them from the so-called Supersoft Sources [Hasinger 1994]) to all sources with SRs ≥ 10.

4. IDENTIFICATION CONTENT OF THE ULTRASOFT SOURCES

Following the same selection criterion for observations as in § 3, we now select all the observations of ultrasoft sources; i.e., those with softness ratio of ≥ 10. These were further divided into identified and unidentified sources. The classification was not restricted to the six classes used in Figures 1 and 3; rather, we used all the identities provided in WGACAT, followed by a search of the SIMBAD database using an error circle of 1′ radius. A list of all the identified ultrasoft objects is given in Table 1, and that of the unidentified ultrasoft sources is given in Table 2. The catalog name, the right ascension (2000), the declination (2000), the observed count rate, and the variability parameter χ^2 (Giommi, White, & Angelini 1995) as given in the WGACAT are listed in the tables. The identities of the sources are also given in Table 1. In Table 2, we give the uncertainty of the source position (error radius) in arcseconds, which depends on the offset of the source from the center of the field, and the values of SRs and HRs. The χ^2 values are for 2 degrees of freedom obtained from a Kolmogorov-Smirnov test performed on all sources using the method described in Giommi et al. (1995). Values greater that 12–15 indicate significant variability. Since the method compares the light curve of the source with that of the entire image, significant χ^2 values might also mean that the background is variable (a rare event in which all bright sources in the image have high χ^2 values). All variability events were, therefore, confirmed individually. Significant variability is confirmed in 13 of the 14 sources with suspected variability. The only unconfirmed case is that of a weak unidentified source, J2200.1−3035. Among these variable sources, seven are known AM Her type CVs, one is a late-type

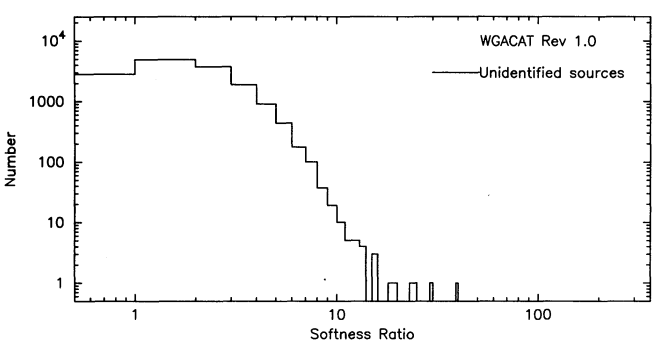

FIG. 2.—Histogram of softness ratio based on ~15,000 observations of unidentified objects detected in the WGACAT. The distribution is broader than in Figs. 1*a* and 1*b*

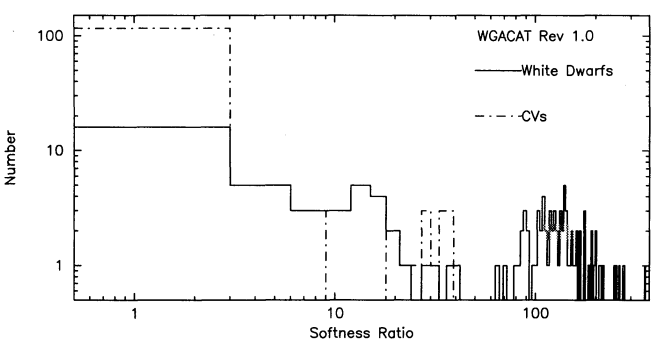

FIG. 3.—Histogram of softness ratios for observations of sources identified with CVs, and white dwarfs. Total number of observations are 138 for CVs, and 124 for WDs. Notice the broad distribution and secondary peaks beyond SR = 10.

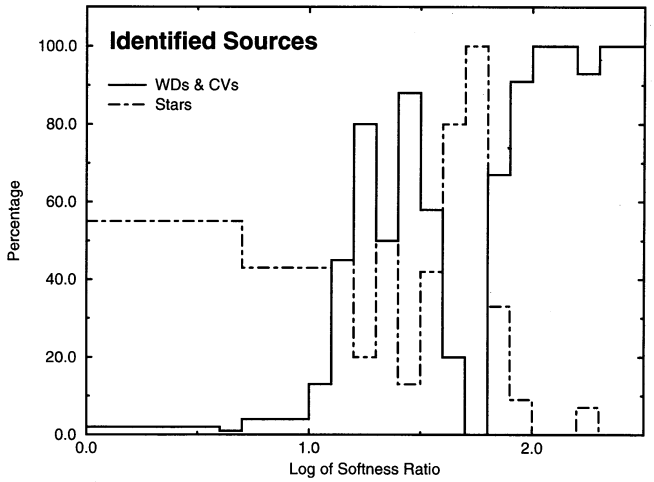

FIG. 4a

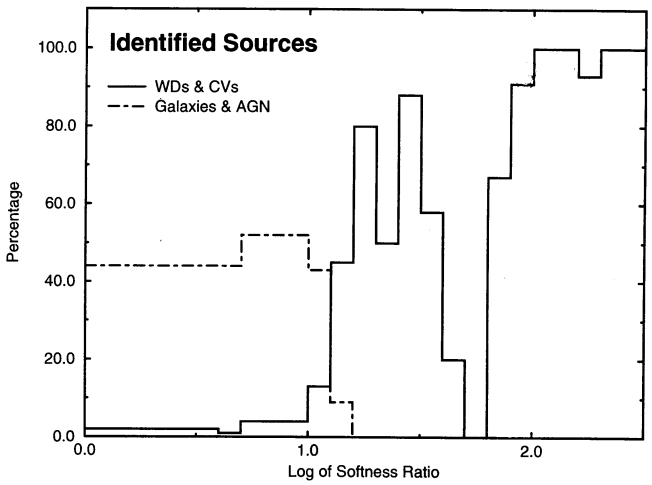

FIG. 4b

FIG. 4.—Percentage distribution of SRs for (*a*) stars vs. CVs and WDs, and (*b*) galaxies and AGNs vs. CVs and WDs, identified in the WGACAT. Notice that the distribution of stars, galaxies and AGNs decreases rapidly near SR = 10, leaving mostly MCVs and WDs at higher SRs.

star, and five are unidentified sources. The unidentified variable sources, therefore, have a good chance of being identified as AM Her type CVs or stars. The light curves of 10 of these sources that have the most interesting variations, including three that are unidentified, are shown in Figure 5.

Some of the weak ultrasoft sources were found, on a closer examination of the images, to be likely "ghost" images (Nousek & Lesser 1993) of nearby bright soft X-ray sources and were deleted from Table 2 and ignored in the following analysis. There are thus, a total of 79 unidentified ultrasoft sources in Table 2. Most of these have well defined image quality expected from a point source; however, some of them have complex morphology due to large offset and therefore, a poorer quality of the point spread function, or are in complex regions of diffuse X-ray emission. These so-called complex sources are J0336.1−2612, J0347.0−1224, J0458.6−3852, J1003.3+4808, J1008.4+3520, J1115.5+1738, J1115.6+4102, J1309.9+3534, J1310.0+3451, J1341.2+4109, J1646.3+5841, J1657.8+4347, and J2200.1−3035.

The observations of all the ultrasoft X-ray sources selected were plotted as SR versus HR color-color diagrams, to better understand their nature. In Figure 6 we show the color-color diagram from observations of all the ultrasoft sources that have been identified with known objects, and similarly in Figure 7 we show all such measurements from 87 observations of 79 unidentified objects. The most prominent classes of objects that can be identified in Table 1 and Figure 6 are the white dwarfs (106 observations of 38 WDs where HZ 43 and 1629+78 were observed 66 times), MCVs (30 observations of 15 CVs), late-type stars (18 observations of nine stars), some early-type stars (one of which is an O star in a planetary nebula), and some unclassified stars (most of which have blue colors). In Figure 6, the WDs occupy the most exclusive region having the softest colors. The MCVs (and a few late-type stars) are somewhat harder. There are, however, some WDs too with a harder spectra that co-exist with the MCVs. The spectral properties of these sources will be discussed in § 5. Apart from these WDs and MCVs, we also find some other interesting types of sources which are briefly discussed below.

1. Three of the supersoft sources discovered in the Magellanic Clouds, viz., J0037.3−7214, J0058.5−7135, and J0439.8−6809 (Hasinger 1994), and a recently discovered Galactic supersoft source, J0019.8+2157 (Beuermann et al. 1995). Only three of the many supersoft sources in the Magellanic Clouds appear in this color-color plot because the high absorption in the direction of the other supersoft sources hardens their observed colors.

2. Three sources associated with other external galaxies viz., FRL 738, KUG 1259+280, and KUG 1331+382. The first one is a compact galaxy with a bright nucleus at a redshift of 0.0591 (Fairall 1984). Its X-ray luminosity of $\sim 2 \times 10^{42}$ ergs s^{-1} is like that of a low-luminosity AGN but with an unusually soft spectrum. The second of these galaxies is a starburst spiral and appears to be in a small group of four galaxies within 1′, and near the Coma cluster. KUG 1259+280 is the brightest among these four galaxies with a magnitude of 15.4 (Takase & Miyauchi-Isobe 1985) and has a heliocentric radial velocity of 7203 km s^{-1}. It is closest to the X-ray source position. The second brightest galaxy, with a magnitude of 17.1 and radial velocity of 6816 km s^{-1}, was earlier identified as an X-ray source in the *EXOSAT* high Galactic latitude survey by Giommi et al. (1991). The other two galaxies in the group are much fainter, and their velocities are unknown. Assuming that the ultrasoft source is associated with KUG 1259+280 we obtain an X-ray luminosity of $\sim 3 \times 10^{42}$ ergs s^{-1} for this source, similar to that of a low-luminosity AGN. KUG 1331+382 is a another spiral galaxy with a magnitude of 17.5 but its radial velocity is not known (Takase & Miyauchi-Isobe 1989). The ultrasoft X-ray source associated with this galaxy could be variable based on another exposure and therefore may signify a highly luminous point source or an AGN in the galaxy. A similarly unusual ultrasoft AGN has recently been found in a Seyfert-type galaxy, Zwicky 159.034 (RE J1237+264), by Brandt, Pounds, & Fink (1995).

3. Four early-type (O–A3) stars, one of which is in a planetary nebula NGC 1360 (Feibelman 1994). This was previously detected by the *EXOSAT* and *Einstein* observatories (Apparao & Tarafdar 1989).

TABLE 1

LIST OF IDENTIFIED ULTRASOFT X-RAY SOURCES IN THE WGACAT

Name (1WGA)	R.A. (2000)	Decl. (2000)	Count Rate (counts s^{-1})	χ^2	Type	Other Names
			White Dwarfs			
J0029.9−6324.....	$00^h29^m56^s.9$	−63°24′59″	0.389 ± 0.0130	8.0	DA	RE J0029−632
J0039.8+3132.....	00 39 52.0	31 32 33	0.046 ± 0.0021	3.3	DA	GD 8, WD 0037+312
J0053.2−3300.....	00 53 17.2	−33 00 02	0.277 ± 0.0094	9.4	DA	GD 659, RE J0053−325
J0118.6−2254.....	01 18 36.4	−22 54 53	0.001 ± 0.0003	1.7	DA	GD 695, WD 0116−231
J0134.4−1607.....	01 34 24.2	−16 07 20	0.188 ± 0.0150	7.1	DA	GD 984, RE J0134−160
J0138.8+2523.....	01 38 52.8	25 23 19	0.080 ± 0.0065	1.0	DA	PG 0136+251, RE J0138+252
J0322.2−5345.....	03 22 14.6	−53 45 11	0.036 ± 0.0015	1.6	DA	BPS CS 22968−036
J0417.1−5457.....	04 17 11.7	−54 57 54	0.003 ± 0.0008	9.9	...	WD 0416−551, EXO 0416.1−5505
J0443.0−0346.....	04 43 05.6	−03 46 16	0.975 ± 0.0150	0.1	DA	RE J0443−034
J0534.3−0213.....	05 34 21.7	−02 13 54	0.008 ± 0.0020	2.7	DA	RE J0534−021
J0550.6+0005.....	05 50 37.1	00 05 47	0.081 ± 0.0045	1.5	DAw	GD 257, RE J0550+000
J0633.7+1041.....	06 33 42.9	10 41 25	0.018 ± 0.0038	1.7	DA	RE J0633+104
J0715.2−7025.....	07 15 16.6	−70 25 10	0.399 ± 0.0120	0.9	DA	RE J0715−702
J0739.3+0513.....	07 39 18.3	05 13 27	1.330 ± 0.0170	0.5	F	GJ 280B, WD 0736+053
J0827.0+2844.....	08 27 05.1	28 44 10	0.068 ± 0.0052	6.2	DA	RE J0827+284
J0907.7+5058.....	09 07 47.2	50 58 19	0.032 ± 0.0028	0.7	DA	PG 0904+511, RE J0907+505
J0916.9−1946.....	09 16 58.0	−19 46 19	0.193 ± 0.0086	5.5	DA	RE J0916−194
J1013.4+0612.....	10 13 27.8	06 12 05	0.014 ± 0.0016	5.5	DA	PG 1010+064
J1032.1+5329.....	10 32 07.5	53 29 20	0.964 ± 0.0110	1.0	DA	RE J1032+532
J1043.5+4454.....	10 43 32.2	44 54 03	0.048 ± 0.0032	0.5	sd:B	PG 1040+451, RE J1043+445
J1146.5+0012.....	11 46 34.8	00 12 23	0.010 ± 0.0015	5.4	DO	WD 1144+004
J1201.7−0345.....	12 01 45.7	−03 45 14	0.029 ± 0.0017	0.2	DO	GW Vir, RE J1201−034
J1236.7+4755.....	12 36 45.6	47 55 29	0.315 ± 0.0120	2.8	sd:B	PG 1234+482, RE J1236+475
J1257.0+2201.....	12 57 02.9	22 01 46	0.375 ± 0.0069	0.7	DAw	GD 153, RE J1257+220, LTT 13724, PG 1254+223
J1316.3+2905.....	13 16 22.5	29 05 57	64.15 ± 0.14	0.4	DAw	HZ 43A,RE J1316+290, WD 1314+293, PG 1314+294
J1406.0−0758.....	14 06 04.8	−07 58 17	0.034 ± 0.0029	4.5	DA	PG 1403−077, WD 1403−077
J1446.0+6329.....	14 46 01.1	63 29 13	0.034 ± 0.0032	0.8	DA F8	RE J1446+632, BD+64°1026
J1502.1+6612.....	15 02 10.3	66 12 11	2.460 ± 0.0230	1.5	DZ	PG 1501+664, RE J1502+661
J1629.1+7804.....	16 29 10.6	78 04 30	0.915 ± 0.0150	0.2	DA	WD 1631+78, RE J1629+780
J1638.4+3500.....	16 38 25.8	35 00 05	0.068 ± 0.0043	1.3	DA	PG 1636+351, RE J1638+350
J1658.8+3418.....	16 58 50.7	34 18 52	0.028 ± 0.0023	1.8	DA	PG 1657+344, WD 1657+343
J1659.8+4400.....	16 59 48.7	44 00 58	0.017 ± 0.0018	3.0	DAp	PG 1658+440, RE J1659+440
J1820.4+5805.....	18 20 24.6	58 05 30	0.196 ± 0.0140	9.8	DA	RE J1820+580
J1821.8+6422.....	18 21 52.0	64 22 00	0.035 ± 0.0045	1.7	PN	DS Dra, RE J1821+642
J2004.2−5602.....	20 04 15.9	−56 02 29	0.009 ± 0.0027	6.3	DA	RE J2004−560, EXO 2000.3−5611
J2013.1+4002.....	20 13 09.2	40 02 14	0.127 ± 0.0069	1.9	DA	RE J2013+400
J2312.3+1047.....	23 12 21.3	10 47 00	0.578 ± 0.0078	0.1	DAw	GD 246, RE J2312+104
J2324.5−5441.....	23 24 31.0	−54 41 35	0.158 ± 0.0065	0.6	DA	RE J2324−544
			Cataclysmic Variables			
J0140.9−6753.....	01 40 58.6	−67 53 24	0.455 ± 0.005	8.0	AM Her	BL Hyi, RE J0141−675
J0335.4−2544.....	03 35 28.0	−25 44 19	(0.24−0.90) ± 0.06	16.0	AM Her	UZ For, EXO 0333.3−2554
J0350.3+1715.....	03 50 21.9	17 15 35	(0.02–0.04) ± 0.01	1.3	WD*	V471 Tau, RE J0350+171
J0453.4−4213.....	04 53 25.6	−42 13 35	(0.16−0.29) ± 0.005	2.9	AM Her	RE J0453−42
J0751.2+1444.....	07 51 17.0	14 44 05	1.960 ± 0.020	1.5	DQ Her	RE J0751+144
J0815.1−1903.....	08 15 06.7	−19 03 09	2.530 ± 0.0130	52.1	AM Her	VV Pup, J0815−190
J1051.5+5404.....	10 51 34.2	54 04 39	(0.375−0.647) ± 0.01	93.7	AM Her	EK UMa, J1051+540
J1104.4+4503.....	11 04 27.3	45 03 38	0.512 ± 0.015	38.0	AM Her	AN UMa, RE J1104+450
J1117.2+1757.....	11 17 15.3	17 57 42	0.055 ± 0.002	12.1	AM Her	DP Leo, 1E 1114.6+1814
J1409.1−4517.....	14 09 06.3	−45 17 24	(2.27−3.35) ± 0.005	1.8	AM Her	V834 Cen, EXO 1405−451
J1816.2+4952.....	18 16 14.0	49 52 18	74.37 ± 0.13	0.5	AM Her	AM Her, 1E 1815.0+4948
J1844.8−7418.....	18 44 48.1	−74 18 36	1.140 ± 0.0180	8.4	AM Her	RE J1844−741
J1938.5−4613.....	19 38 35.7	−46 13 03	0.350 ± 0.0057	4.0	AM Her	RE J1938−461
J2005.6+2240.....	20 05 41.8	22 40 06	1.190 ± 0.0093	36.3	AM Her	QQ Vul, RE J2005+224
J2107.9−0517.....	21 07 58.4	−05 17 36	0.518 ± 0.0077	11.2	AM Her	RE J2107−051
			Late-Type Stars			
J0025.6−7715.....	00 25 38.4	−77 15 23	0.018 ± 0.0027	2.2	G2 IV	HD 2151, β Hyi
J0610.2−7445.....	06 10 15.9	−74 45 06	0.027 ± 0.0034	12.8	G6 V	HD 43834, α Men
J1439.6−6050.....	14 39 38.9	−60 50 23	1.810 ± 0.0240	0.2	G2 V	HD 128621, α Cen
J1538.0+6603.....	15 38 01.1	66 03 32	0.002 ± 0.0006	3.3	K0	BD +66°914, SAO 16793
J1601.6+6648.....	16 01 39.8	66 48 09	0.325 ± 0.0150	1.3	K0	BD +67°922, AG Dra
J1631.9+4358.....	16 31 54.5	43 58 52	0.114 ± 0.0099	1.6	G0	BD +44°2586
J2100.0−4238.....	21 00 05.1	−42 38 48	0.013 ± 0.0015	6.7	K3	CD −43°14304
J2347.7−2610.....	23 47 42.8	−26 10 52	0.024 ± 0.0051	5.8	G8	HD 223219, CD−26°16784
J2339.3+7737.....	23 39 18.9	77 37 10	0.006 ± 0.0011	3.4	K1 III	HD 222404, γ Cep

TABLE 1—*Continued*

Name (1WGA)	R.A. (2000)	Decl. (2000)	Count Rate (counts s^{-1})	χ^2	Type	Other Names
			Early-Type Stars			
J0333.2−2551.....	03 33 13.3	−25 51 56	0.023 ± 0.0026	2.1	O/PN	NGC 1360, PHL 1556
J0648.0−4418.....	06 48 04.6	−44 18 54	0.090 ± 0.0043	0.4	O6p	HD 49798, CD−44°2920
J1104.4+3814.....	11 04 29.7	38 14 15	(0.01–0.013) ± 0.0014	6.0	A3 III	HD 95934, 51 UMa
J1135.8−6301.....	11 35 48.5	−63 01 02	0.041 ± 0.0048	2.4	B9 III	HD 100841, λ Cen
			Unclassified Stars			
J0514.1−4001.....	05 14 06.4	−40 01 22	0.005 ± 0.0008	3.3	...	NGC 1851
J1059.2+5124.....	10 59 16.4	51 24 49	0.742 ± 0.0160	1.5	Blue	LB 1919, RE J1059+512
J1312.5+2832.....	13 12 30.6	28 32 09	0.031 ± 0.0033	0.7	Blue	US 423
J1328.2+3617.....	13 28 14.0	36 17 32	0.025 ± 0.0044	2.7	...	CSO 989
			Super Soft Sources			
J0019.8+2157.....	00 19 49.7	21 57 01	(0.93–1.06) ± 0.01	0.8		Galactic source
J0037.3−7214.....	00 37 18.5	−72 14 03	0.208 ± 0.006	7.5		SMC (WW 13), 1E 0035.4−7230
J0058.5−7135.....	00 58 35.7	−71 35 43	0.249 ± 0.005	0.2		SMC (WW 43), 1E 0056.8−7154
J0439.8−6809.....	04 39 50.3	−68 09 08	0.584 ± 0.015	0.4		LMC source
			Galaxies and AGNs			
J0308.5−4743.....	03 08 35.8	−47 43 29	0.011 ± 0.0018	0.8		FRL 738
J1301.9+2746.....	13 01 59.5	27 46 51	0.086 ± 0.0030	1.7	S0/Sp	KUG 1259+280, EXO 1259.6+2803
J1334.1+3800.....	13 34 11.0	38 00 21	0.005 ± 0.0013	8.2	S	KUG 1331+382
J1336.7+2721.....	13 36 47.0	27 21 18	0.005 ± 0.0011	1.9	QSO	1334.5+2736
J1342.3+2720.....	13 42 21.3	27 20 58	0.017 ± 0.0036	1.5	QSO	1340+275
			Assorted Types			
J0633.9+1746.....	06 33 54.3	17 46 12	0.214 ± 0.0075	2.1	Pulsar	Geminga, 1E 0630.9+1748
J1959.6+2243.....	19 59 36.6	22 43 26	(0.034–0.045) ± 0.0027	3.2	PN	Dumbbell, M27, NGC 6853, RE J1959+224
J2004.3−5543.....	20 04 19.0	−55 43 24	(0.043–0.057) ± 0.005	2.7	Nova	RR Tel, IRAS 20003−5552

NOTES.—The χ^2 is the variability parameter in the WGACAT (see text). The variability seen in different observations is indicated as the range of values in cols. (4) and (5). RE: EUV source (Pye et al. 1995); 1E: *Einstein* X-ray source (Harris et al. 1990; Plummer et al. 1991); EXO: *EXOSAT* source (Giommi et al. 1991).

4. The planetary nebula known as the Dumbbell (NGC 6853, M27), the X-ray emission from which is most probably extended (Kreysing et al. 1992).

5. A well known symbiotic nova: RR Tel (Allen 1981).

6. The Geminga pulsar (Halpern & Holt 1992), with a very soft blackbody component and low N_H.

7. Two QSOs in an extended field around 1338+27, both of which are weak emission-line objects in a spectroscopic survey of quasars in that field (Crampton et al. 1988). The brighter of the two QSOs, J1342.3+2720, has a magnitude of 17.2 and is at a redshift of 0.704. The other object, J1336.7+2721, is of 19.4 magnitude and a redshift of 1.95.

5. UNIDENTIFIED ULTRASOFT SOURCES AND THEIR LIKELY SPECTRAL PROPERTIES

To further learn about the sources in Table 2 and Figure 7 (also see Table 1 and Fig. 6), we have investigated their general spectral properties by simulating the SRs and HRs expected for some standard types of spectral models. We choose to present SRs and HRs for the models that can be appropriately used for a variety of objects listed in Table 1. These models are

1. Blackbody emission or thermal plasma emission models at different temperatures (Raymond & Smith 1978; Raymond 1990), useful for WDs, MCVs, and late-type stars.

2. Power laws of varying photon index (Γ), useful for AGNs.

3. A power law with flat (Γ = 1) slope, having various exponential cutoff energies (cutoff power law), and four edges at 0.391, 0.487, 0.665, and 0.758 keV for mimicking the emission from a white dwarf atmosphere (Heise 1995).

4. Combinations of a blackbody and a very hot (kT = 25 keV) thermal bremsstrahlung component as is characteristic of the spectra of MCVs. In this example, the normalizations of both components were kept equal.

A cold absorber model for the interstellar medium assuming absorption cross sections given by Morrison & McCammon (1983) was used along with each of the above models. The colors generated from such simulations for different values of intervening interstellar absorption columns (N_H) ranging from 0.1–30.0 × 10^{19}cm^{-2} are shown in Figures 8*a*–8*d* and can be directly compared with those of Figures 6 and 7. The range of other parameters that produce the colors shown in Figures 8*a*–8*d* are (1) a kT of 45 (60 eV) to 90 eV (120 eV) for blackbody temperature (plasma emission temperature) (Figs. 8*a* and 8*b*), (2) a Γ of 2–10 for the power laws (Fig. 8*c*), (3) an exponential cutoff energy of 90–400 eV (Fig. 8*d*), and (4) a kT of 15–75 eV for the blackbody temperature in the two-component spectra (Fig. 8*a*). For lower values of kT in parameters 1 and 3, and higher values of Γ in parameter 2 above, the SR continues to rise but the HR drops very rapidly. Because of the limited range of the log scale on the *y*-axis in Figures 8*a*–8*d*, this range is not fully represented in the figures.

TABLE 2

LIST OF UNIDENTIFIED ULTRASOFT X-RAY SOURCES IN THE WGACAT

Name (1WGA)	R.A. (2000)	Decl. (2000).	Error Radius	Count Rate (counts s^{-1})	SR	HR	χ^2
J0016.0−3914.....	$00^h16^m01^s0$	−39°14′36″	13	0.0045 ± 0.0006	10.9 ± 3.4	0.18 ± 0.14	2.0
J0139.2−5430.....	01 39 13.4	−54 30 05	13	0.0124 ± 0.0015	13.9 ± 4.3	0.27 ± 0.18	1.5
J0205.7−1337.....	02 05 45.9	−13 37 53	50	0.0536 ± 0.0059	16.5 ± 3.4	0.6 ± 0.2	1.3
J0309.3−4741.....	03 09 19.8	−47 41 39	50	0.0050 ± 0.0012	10.6 ± 5.0	2.4 ± 1.3	1.8
J0335.5−3449.....	03 35 34.4	−34 49 58	13	0.0280 ± 0.0016	74 ± 17	0.25 ± 0.12	19.1
J0336.1−2612.....	03 36 07.9	−26 12 07	50	0.0096 ± 0.0019	11.7 ± 3.9	1.5 ± 0.6	8.8
J0347.0−1224.....	03 47 04.1	−12 24 42	50	0.0041 ± 0.0012	10.3 ± 4.1	1.4 ± 0.7	2.4
J0406.4−3112.....	04 06 29.1	−31 12 31	50	0.0070 ± 0.0017	10.7 ± 3.7	1.8 ± 0.7	0.5
J0415.5−1140.....	04 15 35.3	−11 40 34	13	0.0033 ± 0.0008	11.6 ± 4.6	0.0	2.0
J0447.9−4403.....	04 47 57.5	−44 03 01	70	0.0079 ± 0.0015	10.2 ± 3.6	1.4 ± 0.63	0.7
J0453.4−4213.....	04 53 25.6	−42 13 35	13	(0.16–0.30) ± 0.005	(36–40) ± 4.0	(0.14–0.28) ± 0.06	2.9
J0458.6−3852.....	04 58 36.8	−38 52 33	50	0.0067 ± 0.0015	21.5 ± 9.0	2.0 ± 1.0	1.6
J0505.6+0158.....	05 05 38.4	01 58 28	50	0.0343 ± 0.0025	13.1 ± 1.7	0.63 ± 0.12	1.5
J0633.3−2311.....	06 33 22.0	−23 11 10	50	0.0135 ± 0.0013	15.6 ± 3.3	0.38 ± 0.15	2.4
J0639.4−6224.....	06 39 29.7	−62 24 09	50	0.1210 ± 0.0081	15.9 ± 3.0	0.24 ± 0.10	58.3
J0800.4−4745.....	08 00 24.5	−47 45 57	13	0.2890 ± 0.0110	31.7 ± 5.0	0.0	3.0
J0803.7−4748.....	08 03 44.6	−47 48 30	50	0.2570 ± 0.0140	13.3 ± 2.0	0.21 ± 0.07	22.1
J0854.0+1336.....	08 54 01.9	13 36 36	50	0.0115 ± 0.0010	14.1 ± 3.2	0.9 ± 0.3	1.2
J0855.9+1812.....	08 55 54.5	18 12 13	50	0.0781 ± 0.0066	11.2 ± 1.6	0.61 ± 0.14	0.6
J0959.6−2603.....	09 59 37.3	−26 03 55	50	(0.048–0.076) ± 0.004	(12–25) ± 1.5	(0.3–0.7) ± 0.06	2.5
J1003.3+4808.....	10 03 22.6	48 08 49	50	0.0346 ± 0.0078	12.0 ± 5.1	2.8 ± 1.3	4.3
J1007.5−2017.....	10 07 34.9	−20 17 24	13	0.1940 ± 0.0044	12.5 ± 0.8	0.24 ± 0.03	4.1
J1008.4+3520.....	10 08 25.9	35 20 11	50	0.0119 ± 0.0028	10.4 ± 2.6	1.1 ± 0.4	3.6
J1008.9+5224.....	10 08 54.3	52 24 09	50	0.0044 ± 0.0010	10.4 ± 3.3	2.4 ± 0.8	3.2
J1011.1+5259.....	10 11 09.3	52 59 28	13	0.0023 ± 0.0007	12.4 ± 5.8	3.0 ± 1.5	4.6
J1019.7+5225.....	10 19 43.2	52 25 33	50	0.0035 ± 0.0008	13.3 ± 5.6	1.8 ± 0.9	2.7
J1028.2+5340.....	10 28 16.9	53 40 31	13	0.0024 ± 0.0005	10.5 ± 4.5	0.5 ± 0.3	2.6
J1042.3+5549.....	10 42 20.3	55 49 18	50	0.0195 ± 0.0040	12.0 ± 5.6	2.8 ± 1.5	6.0
J1047.1+6335.....	10 47 09.5	63 35 11	50	(0.035–0.05) ± 0.003	(20–25) ± 4.0	(0.3–0.9) ± 0.2	0.7
J1053.6+5358.....	10 53 36.4	53 58 18	50	0.0027 ± 0.0007	10.0 ± 4.7	1.2 ± 0.7	3.9
J1106.4+6050.....	11 06 24.7	60 50 14	50	0.0042 ± 0.0008	10.9 ± 3.0	1.5 ± 0.5	2.1
J1108.6+4521.....	11 08 41.3	45 21 29	50	0.0084 ± 0.0024	10.0 ± 4.7	1.0 ± 0.6	3.4
J1115.5+1738.....	11 15 34.5	17 38 21	50	0.0050 ± 0.0010	10.2 ± 1.9	0.9 ± 0.2	1.1
J1115.6+4102.....	11 15 41.6	41 02 26	50	0.0048 ± 0.0011	12.5 ± 3.2	1.4 ± 0.4	2.0
J1118.0+1830.....	11 18 04.5	18 30 59	50	0.0093 ± 0.0012	10.6 ± 1.8	0.7 ± 0.2	1.6
J1209.3+0953.....	12 09 21.3	09 53 27	50	0.0066 ± 0.0016	10.3 ± 3.6	0.4 ± 0.3	0.8
J1210.2+3856.....	12 10 15.8	38 56 04	50	0.0102 ± 0.0028	10.0 ± 4.3	0.8 ± 0.5	1.7
J1215.5+3305.....	12 15 33.7	33 05 46	13	0.0025 ± 0.0004	10.0 ± 4.3	2.8 ± 1.3	1.8
J1219.7+3407.....	12 19 45.7	34 07 37	50	(0.022–0.046) ± 0.004	(12–19) ± 4.1	(0.4–1.0) ± 0.3	0.1
J1221.8+0350.....	12 21 51.2	03 50 44	50	0.0091 ± 0.0016	10.4 ± 3.3	1.5 ± 0.6	1.4
J1229.4+2416.....	12 29 29.9	24 16 02	50	0.0187 ± 0.0051	13.6 ± 6.3	1.2 ± 0.7	4.0
J1236.9+2656.....	12 36 57.0	26 56 50	13	0.0199 ± 0.0024	11.0 ± 3.5	0.9 ± 0.4	28.0
J1249.8+2558.....	12 49 48.8	25 58 51	50	0.0163 ± 0.0044	10.2 ± 4.8	1.8 ± 1.0	1.1
J1256.4−0613.....	12 56 25.1	−06 13 59	50	0.0067 ± 0.0022	10.7 ± 5.6	1.0 ± 0.7	2.9
J1309.9+3534.....	13 09 56.1	35 34 16	50	0.0102 ± 0.0026	10.2 ± 3.1	1.2 ± 0.5	5.3
J1310.0+3451.....	13 10 00.9	34 51 29	50	0.0248 ± 0.0037	10.6 ± 2.3	1.1 ± 0.3	2.0
J1332.8+0133.....	13 32 48.6	01 33 20	50	0.0165 ± 0.0019	10.8 ± 2.5	1.0 ± 0.3	1.1
J1334.0+5117.....	13 34 00.3	51 17 42	50	0.0319 ± 0.0042	10.9 ± 3.0	0.9 ± 0.3	3.0
J1339.8+4015.....	13 39 53.6	40 15 52	50	0.0103 ± 0.0021	10.0 ± 2.8	1.1 ± 0.4	2.3
J1340.8+5128.....	13 40 52.6	51 28 17	50	0.0052 ± 0.0009	10.7 ± 2.6	1.8 ± 0.5	1.0
J1341.2+4109.....	13 41 15.7	41 09 51	50	0.0102 ± 0.0018	11.0 ± 3.5	1.7 ± 0.6	9.8
J1342.6+4024.....	13 42 39.2	40 24 33	13	(0.006–0.017) ± 0.0014	(3.4–11.4) ± 1.0	(0.6–2.0) ± 0.3	8.2
J1342.6+3512.....	13 42 41.2	35 12 33	50	0.0117 ± 0.0023	10.3 ± 3.6	0.8 ± 0.4	5.0
J1344.8+5602.....	13 44 49.8	56 02 16	13	0.0013 ± 0.0004	10.4 ± 4.7	2.8 ± 1.5	2.6
J1427.9+4720.....	14 27 55.4	47 20 29	50	0.0071 ± 0.0019	12.9 ± 5.0	1.0 ± 0.5	1.5
J1443.9+5227.....	14 43 58.9	52 27 02	50	0.0050 ± 0.0015	10.4 ± 4.9	2.8 ± 1.5	2.2
J1511.7+3343.....	15 11 44.8	33 43 32	50	0.0044 ± 0.0012	10.7 ± 4.6	2.3 ± 1.1	4.7
J1522.9+6604.....	15 22 56.0	66 04 50	13	0.0674 ± 0.0040	57.1 ± 16.0	0.1 ± 0.1	5.8
J1547.0−3644.....	15 47 00.7	−36 44 59	50	(0.115–0.135) ± 0.021	(11–14) ± 2.4	0.7 ± 0.2	2.9
J1621.3+6119.....	16 21 20.7	61 19 13	50	0.0062 ± 0.0013	10.0 ± 4.0	0.9 ± 0.5	3.6
J1622.3+4627.....	16 22 19.8	46 27 44	50	0.0110 ± 0.0028	10.0 ± 4.0	0.6 ± 0.4	1.8
J1622.9+4639.....	16 22 59.5	46 39 28	50	0.0128 ± 0.0037	15.3 ± 6.5	1.3 ± 0.7	7.0
J1625.5+4043.....	16 25 35.3	40 43 35	50	0.0084 ± 0.0014	10.7 ± 3.2	2.4 ± 0.8	3.8
J1626.4+4114.....	16 26 25.5	41 14 51	50	0.0037 ± 0.0010	16.0 ± 7.4	1.6 ± 0.9	1.5
J1628.9+4008.....	16 28 58.3	40 08 29	50	(0.29–0.37) ± 0.013	(9.5–10.5) ± 0.5	(0.5–0.6) ± 0.04	0.3
J1630.7+4020.....	16 30 42.2	40 20 00	50	0.0056 ± 0.0017	10.8 ± 5.0	1.0 ± 0.6	3.0
J1644.9+3849.....	16 44 56.9	38 49 16	50	0.0059 ± 0.0018	11.3 ± 4.4	0.7 ± 0.4	2.5
J1646.3+5841.....	16 46 19.4	58 41 28	50	0.0094 ± 0.0019	11.0 ± 4.1	1.2 ± 0.6	2.0
J1657.8+4347.....	16 57 50.6	43 47 47	50	0.0092 ± 0.0019	10.1 ± 3.5	1.2 ± 0.5	2.4
J1701.4+6044.....	17 01 24.3	60 44 59	50	0.0041 ± 0.0009	11.6 ± 4.0	1.8 ± 0.7	2.8

TABLE 2—*Continued*

Name (1WGA)	R.A. (2000)	Decl. (2000).	Error Radius	Count Rate (counts s^{-1})	SR	HR	χ^2
J1757.8+0440.....	17 57 48.6	04 40 15	13	0.0094 ± 0.0017	10.0 ± 4.0	0.6 ± 0.4	15.7
J1802.1+1804.....	18 02 06.4	18 04 48	13	(0.4–3.3) ± 0.03	(20–22) ± 1.0	(0.1–0.8) ± 0.04	6.4
J1856.5−3754.....	18 56 35.4	−37 54 40	13	1.8700 ± 0.0200	10.0 ± 0.3	0.02 ± 0.004	0.1
J2131.3+7036.....	21 31 18.5	70 36 51	13	0.0035 ± 0.0006	11.9 ± 4.7	0.3 ± 0.2	4.7
J2153.3−1514.....	21 53 19.6	−15 14 27	50	0.0200 ± 0.0020	10.7 ± 1.5	0.8 ± 0.2	3.3
J2200.1−3035.....	22 00 09.7	−30 35 36	50	0.0105 ± 0.0021	14.0 ± 4.8	1.8 ± 0.7	13.8
J2216.2−3022.....	22 16 16.0	−30 22 31	50	0.0062 ± 0.0013	10.5 ± 3.2	0.9 ± 0.4	1.8
J2304.7−3514.....	23 04 45.7	−35 14 59	13	0.0032 ± 0.0008	11.4 ± 5.3	0.2 ± 0.2	1.7
J2314.7−4948.....	23 14 42.3	−49 48 04	13	0.0051 ± 0.0007	16.1 ± 5.9	1.0 ± 0.5	3.2

NOTES.—The χ^2 is the variability parameter in the WGACAT, based on a single observation. The variability seen in different observations is indicated as the range of values in cols. (4) and (5). Fourteen sources have poorly defined image due to the deterioration of the point spread function off-axis, or due to the presence of complex emission. These are listed in the text in § 4.

A general feature for all types of spectra in Figures 8*a*–8*d* is that SRs decrease with increasing N_H. Therefore, one immediate result of comparison of Figure 8 with Figures 6 and 7 is that, for most ultrasoft sources the N_H must be quite low ($\leq 10^{19}$ cm^{-2}). This is consistent with the distribution of these sources in the Galactic coordinates which shows that nearly all the unidentified sources avoid the Galactic plane and the Galactic center regions, being at latitudes $|b| \geq 10°$. Some of the identified sources which are at lower Galactic latitudes are known to be nearby. Second, for models 1–3 above, the SR decreases with increasing kT for model 1, decreasing Γ for model 2, and increasing cutoff energy for model 3. For the two-component spectra as in model 4, the HR decreases whereas the SR first increases and then decreases, as the blackbody temperature increases. This leads to the following results:

For sources with SRs $\geq$ 100 but with negligible HRs, if represented by the thermal spectra, the N_H must be $\leq 10^{19}$ cm^{-2} and the kT also must be very low, e.g., for an RS plasma with kT of 45 eV and $N_H = 0.1 \times 10^{19}$ cm^{-2}, SR = 119 and HR $\simeq$ 0. However, in the case of a power law, N_H can be up to 30×10^{19} cm^{-2} but the spectrum is still required to be very steep ($\Gamma \geq 4$). Most sources in this region are WDs (see Fig. 6). For sources with SRs $\leq$ 100 there are many more possibilities depending on their values of HR. For HRs $\leq$ 0.1 similarly steep models with higher N_H are needed. For higher values of HR, the sources in Figures 6 and 7 cannot have spectra consisting of a single-component blackbody or thermal plasma. Such sources could have a power-law type spectra which is somewhat flatter, $\Gamma = 2.0$–4.0, or cutoff power law resembling a WD atmosphere. In either case, a wide range of values for N_H of 0.1–30.0×10^{19} cm^{-2} would be possible. Other possible spectra for such sources are two-component spectra of which we give one example, the combination of a blackbody and thermal bremsstrahlung. The last of these is taken to represent MCVs, and in fact, overlaps the same range in the color-color plots that is occupied by the MCVs in Figure 6. A comparison of Figure 6 with Figures 8*a*–8*d* shows that there are some WDs that have SRs $\geq$ 100 and HRs of $\sim$0.5, a region avoided by the models used by us in Figures 8*a*–8*d*. This could be due to either a larger error in the observed values of the HRs of these sources which are particularly sensitive to the background subtraction or the failure of the coarse models used to mimic the WD atmospheres. Most of the unidentified sources (see Fig. 7) appear to have SRs in the range of 10–30 and HRs $\geq$ 0.1; thus their X-ray spectra either need to be of a composite nature like that of MCVs or have less steep power laws ($\Gamma \leq 2.0$) and moderate N_H.

6. CONCLUSIONS

We have used broadband X-ray colors to isolate the softest population of X-ray sources detected in 3 years of *ROSAT* PSPC pointings.

In most cases, the extreme softness of these sources is due to a very low column density in their direction, as a consequence, most of the low Galactic latitude sources are expected to be nearby. The softest among these sources have been identified with white dwarfs. The other sources mostly represent polar-type CVs or late-type stars. Although our selection criterion is efficient in picking up white dwarfs, MCVs, late-type stars, and unusual AGNs, it does not pick up all such objects, and all such objects do not necessarily have ultrasoft spectra. A few examples of luminous soft sources in external galaxies also show up in our sample and may have some extremely interesting and unusual properties. This list of unidentified sources probably contains many MCVs, WDs, AGNs, and, possibly, a new class of objects with composite spectra. Follow-up optical study of these unidentified ultrasoft sources is now required. Most of them have no optical counterpart in the Guide Star Catalog (GSC), which suggests that they are typically fainter than 16th magnitude. It should, however, be borne in mind that the GSC is not a complete list of stars brighter than 16th magnitude and hence brighter objects may be found in the error circles of this unidentified population. An application of similar selection criteria to the *ROSAT* Sky Survey data should reveal many more such objects.

We thank Steve Fantasia for providing the variability curves, and Steve Drake for his general comments and suggestions. This research has made use of *ROSAT* archival data obtained through the High Energy Astrophysics Science Archive Research Center, HEASARC, Online Service, provided by the NASA-Goddard Space Flight Center. The HEASARC database, the Simbad database, operated at CDS, Strasbourg, France; and the NASA/IPAC Extragalactic Database (NED) which is operated by the Jet Propulsion Laboratory, Caltech, under contract with the NASA were used to identify some of the objects.

1995ApJ...455..456S

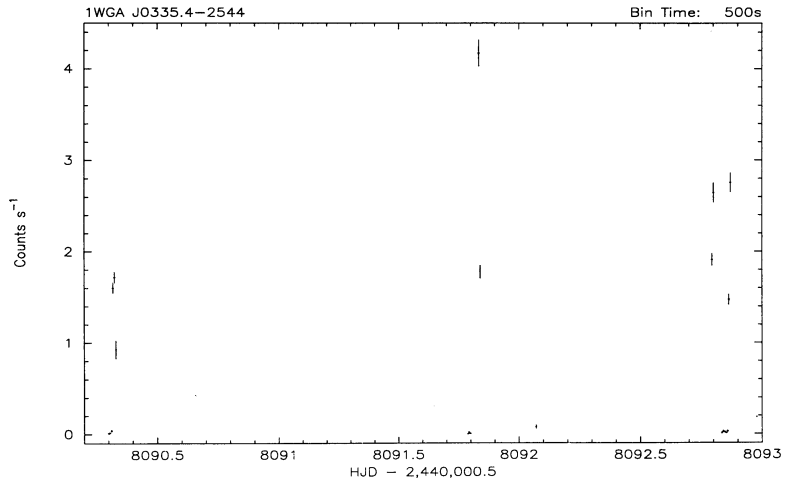

FIG. 5*a*

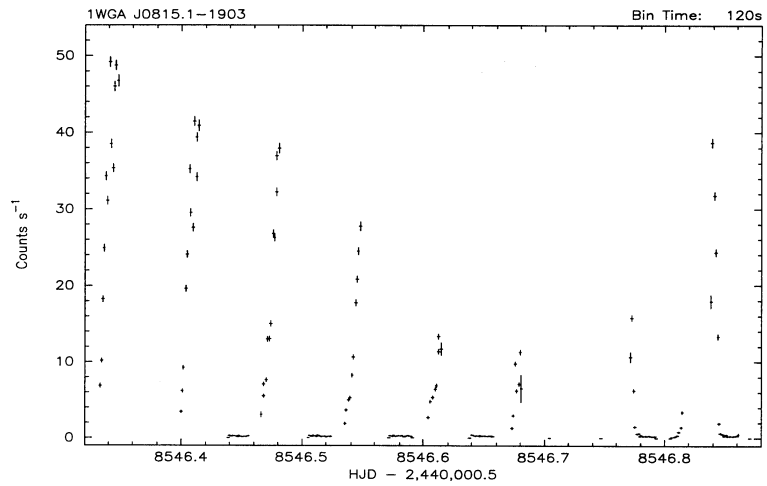

FIG. 5*b*

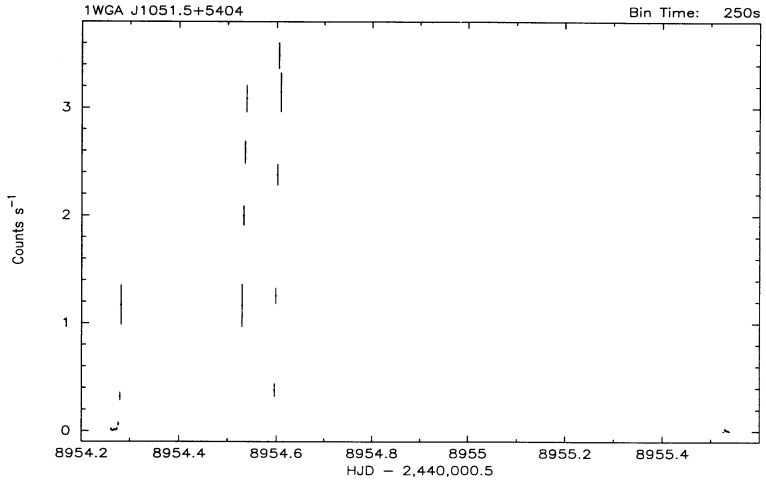

FIG. 5*c*

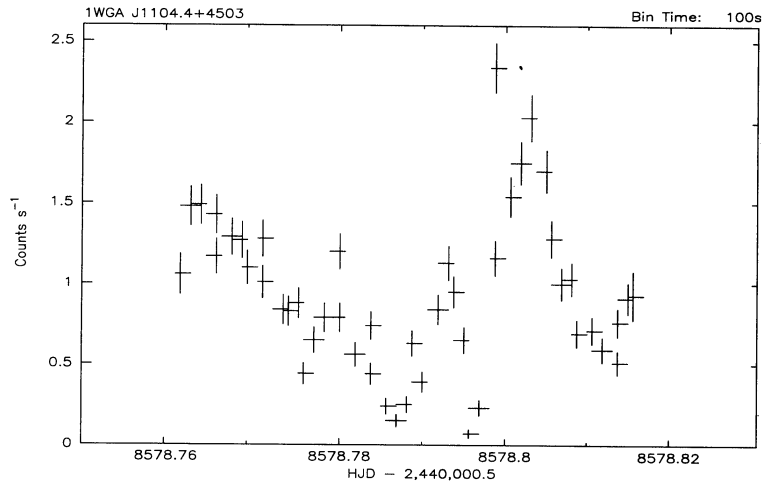

FIG. 5*d*

FIG. 5.—X-ray light curves of the variable sources: (*a*) UZ For, (*b*) VV Pup, (*c*) EK UMa, (*d*) AN UMa, (*e*) DP Leo, (*f*) QQ Vul, (*g*) New AM Her type: J2107.9−0517, (*h*) J0639.4−6224, (*i*) J0803.7−4748, and (*j*) J1236.9+2656. The last three sources are unidentified.

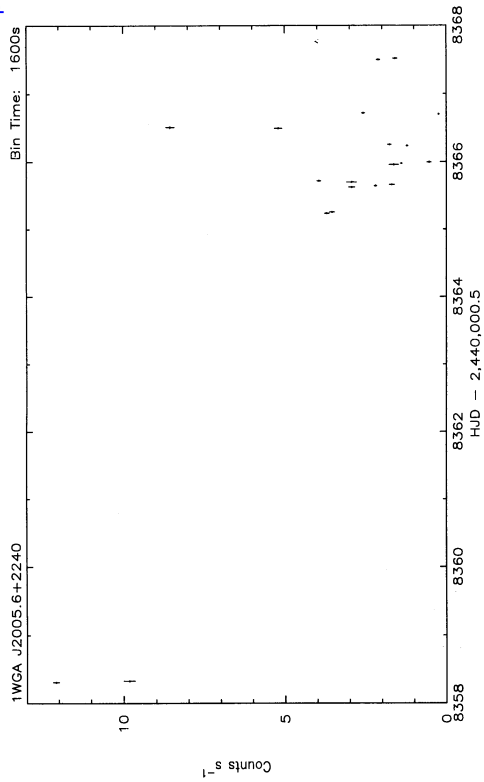

FIG. 5*f*

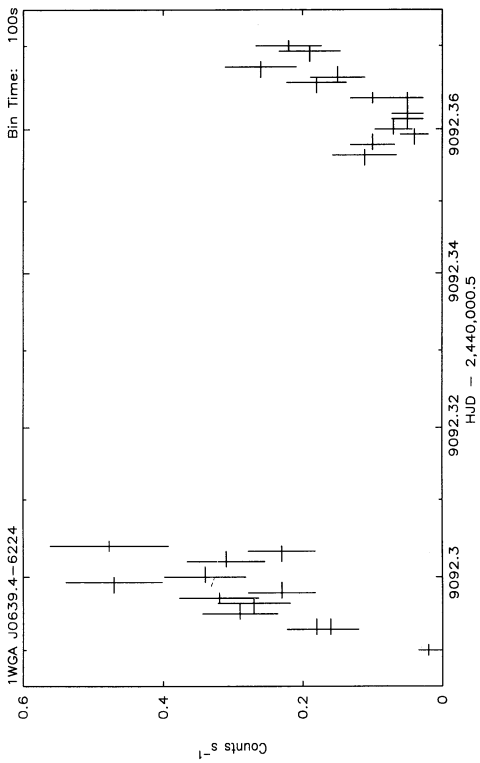

FIG. 5*h*

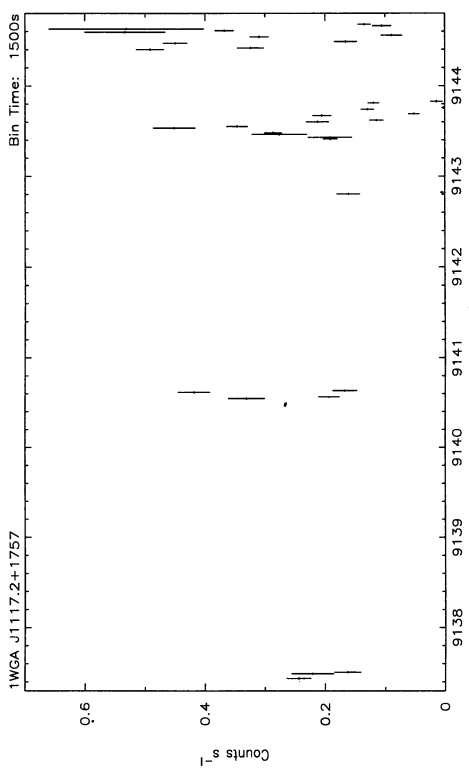

FIG. 5*e*

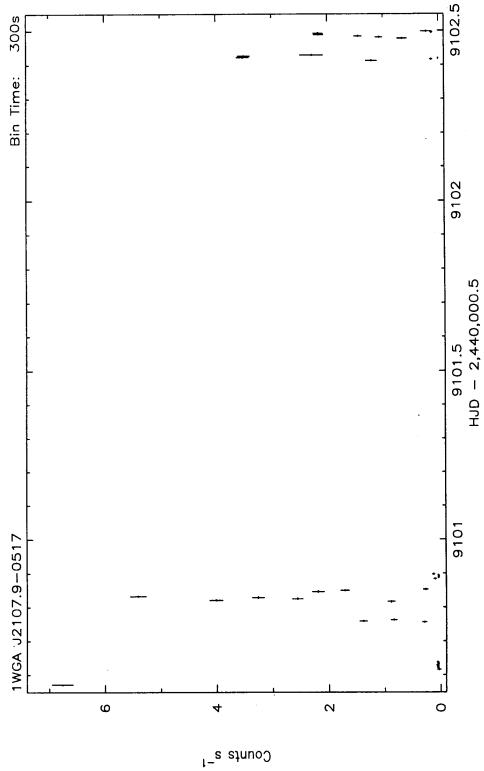

FIG. 5*g*

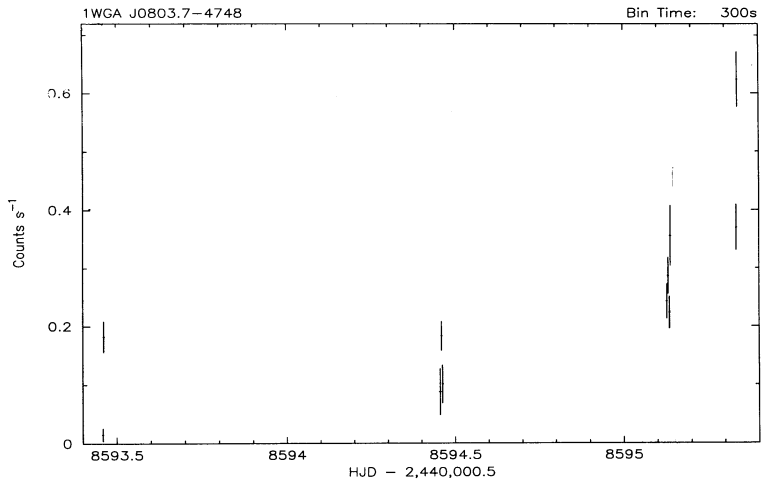

FIG. 5*i*

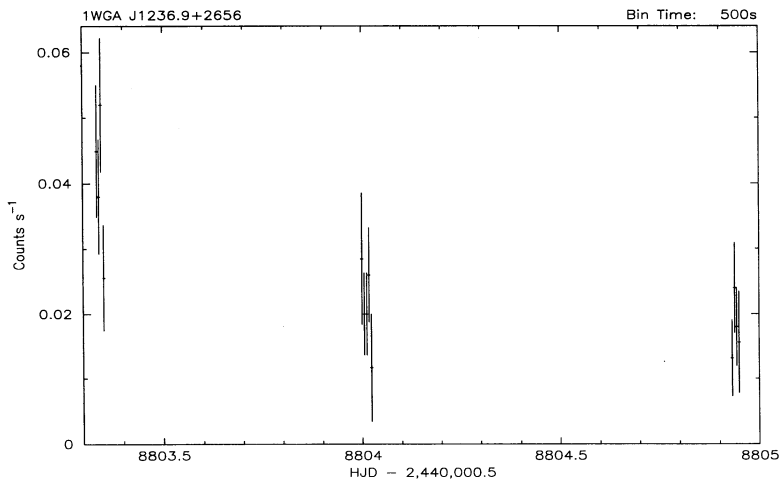

FIG. 5*j*

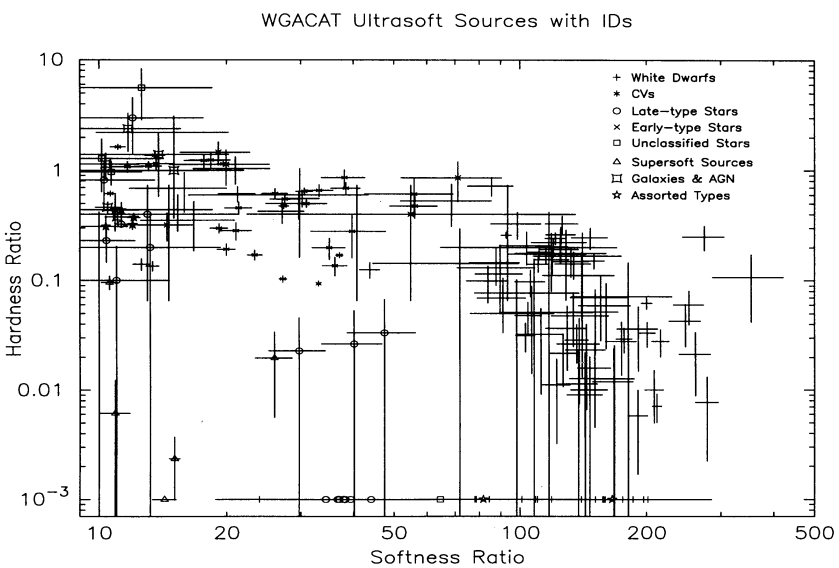

FIG. 6.—SR vs. HR color-color diagram of the identified ultrasoft (SRs $\geq$ 10) X-ray sources. Total number of objects of each class and the number of data points plotted are WDs (38, 106), CVs (15, 30), late-type stars (9, 18), early-type stars (4, 6), unclassified stars (4, 4), supersoft sources (4, 5), galaxies and AGNs (5, 6), and assorted types (3, 7). The first number in the parentheses is the number of objects (also see text).

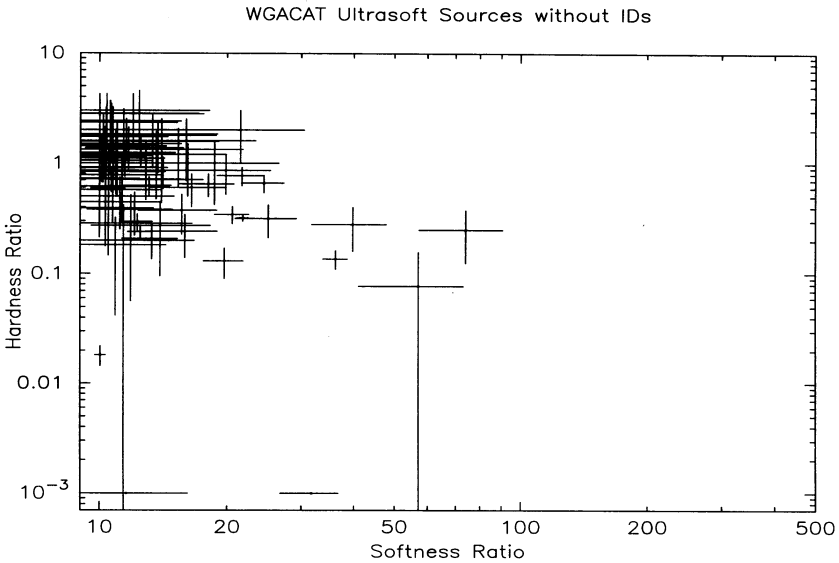

FIG. 7.—Same as in Fig. 6 for the unidentified ultrasoft X-ray sources

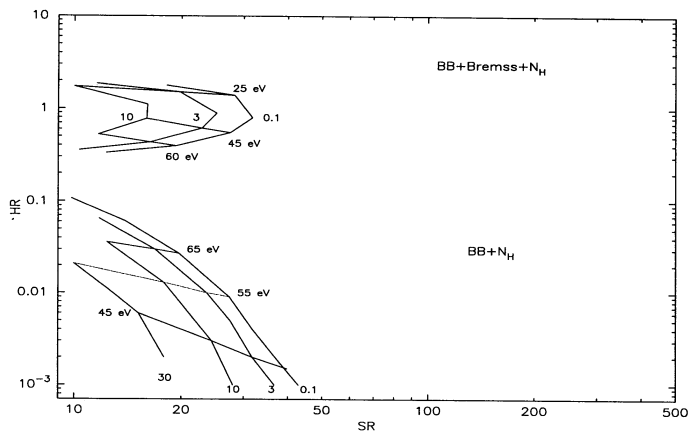

FIG. 8*a*

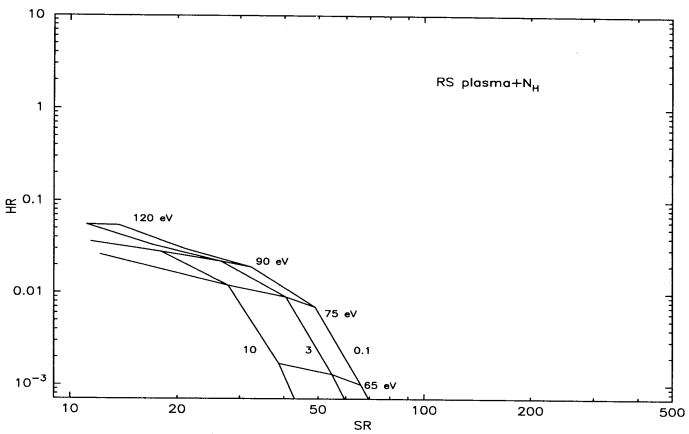

FIG. 8*b*

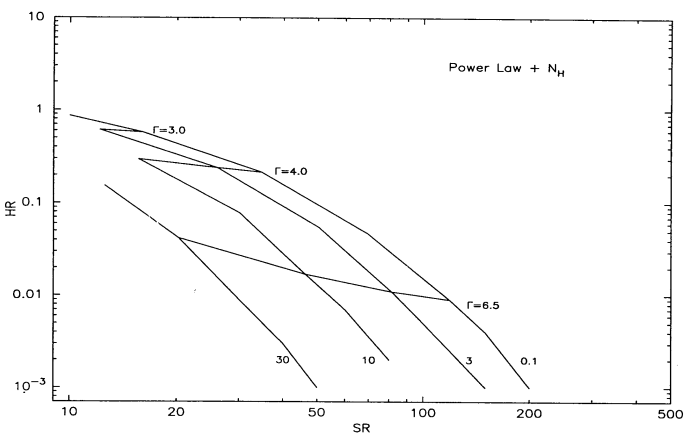

FIG. 8*c*

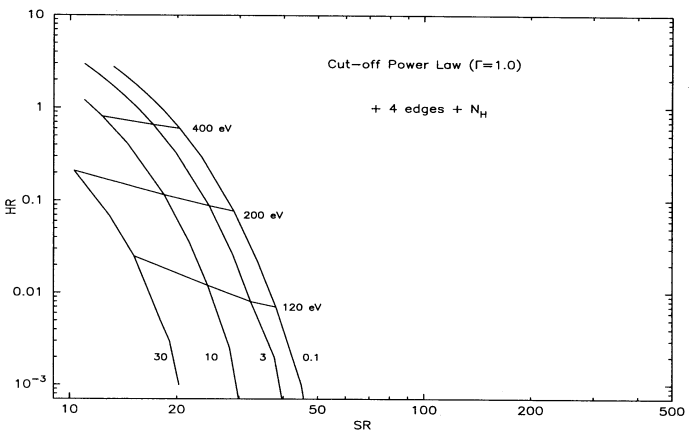

FIG. 8*d*

FIG. 8.—Simulated colors for five types of spectra of ultrasoft sources. Different curves represent different values of N_H (0.1, 3, 10, 30) in units of 10^{19} cm^{-2}. (*a*) A blackbody, and combinations of a blackbody and thermal bremsstrahlung. (*b*) Thermal plasma emission. (*c*) Simple power laws. (*d*) Cutoff power laws mimicking the WD atmosphere. The variables along the curves are blackbody temperature in eV for (*a*), plasma temperature in eV for (*b*), photon index (Γ) for (*c*), and exponential cutoff in eV for (*d*).

REFERENCES

Allen, D. A. 1981, MNRAS, 197, 739
Apparao, K. M. V., & Tarafdar, S. P. 1989, ApJ, 344, 826
Barstow, M. A., et al. 1993, MNRAS, 267, 647
Beuermann, K., et al. 1995, A&A, 294, L1
Brandt, W. N., Pounds, K. A., & Fink, H. 1995, MNRAS, 273, L47
Crampton, D., Cowley, A. P., Schmidtke, P. C., Janson, T., & Durrel, P. 1988, AJ, 96, 816
Fairall, A. P. 1984, MNRAS, 210, 69
Feibelman, W. A. 1994, PASP, 106, 756
Giommi, P., White, N. E., & Angelini, L. 1995, in ASP Conf. Ser., Vol. 77, Astronomical Data Analysis Software and Systems. IV., ed. H. Payne & J. Hayes (San Francisco: ASP), 117
Giommi, P., et al. 1991, ApJ, 378, 77
Halpern, J. P., & Holt, S. S. 1992, Nature, 357, 222
Harris, D.E., et al. 1990, The *Einstein Observatory* Catalog of IPC X-Ray Sources (CD-ROM Version, 1990 January 1)
Hasinger, G. 1994, in AIP Conf. Proc., No. 308, The Evolution of X-Ray Binaries, ed. S. S. Holt & C. S. Day (New York: AIP), 611
Heise, J. 1995, private communication.
Kreysing, H. C., Diesch, C., Zweigle, J., Staubert, R., Grewing, M., & Hasinger, G. 1992, A&A, 264, 623
McCook, G. P., & Sion, E. M. 1987, ApJS, 65, 603
Morrison R., & McCammon, D. 1983, ApJ, 270, 119
Nousek, J., & Lesser, A. 1993, *ROSAT* Newsletter, 8, 13
Pfeffermann, E., et al. 1987, Proc. SPIE, 733, 519
Plummer, D., Schachter, J., Garcia, M., & Elvis, M. 1991, The *Einstein Observatory* IPC Slew Survey Catalog (CD-ROM Version, 1991 January 1)
Pye, J. P., et al. 1995, MNRAS, 274, 1165
Raymond, J. C. 1990, private communication
Raymond, J. C., & Smith, B. W. 1978, ApJS, 35, 419
Shara, M. M., Shara, D. J., & McLean, B. 1993, PASP, 105, 387
Takase, B., & Miyauchi-Isobe, N. 1985, Ann. Tokyo Astron. Obs., 20, 237
———. 1989, Pub. Natl. Astron. Obs. Japan, 1, 11
Trümper, J. 1983, Adv. Space Res., 2, 241
van den Heuval, E. P. J., Bhattacharya, D., Nomoto, K., & Rappaport, S. A. 1992, A&A, 262, 97
White, N. E., Giommi, P., & Angelini, L. 1994, IAU Circ., No. 6100 (Also, URL: http://legacy.gsfc.nasa.gov/ white/wgacat/wgacat.html)
White, N.E., Giommi, P., Heise, J., Angelini, L., & Fantasia, S. 1995, ApJ, 445, L125

Note added in proof.—After the paper was accepted, several objects in Table 2 were identified optically and are listed here (the details will be published elsewhere). From the digitized sky survey, J0016.0−3914 could be a "supersoft" X-ray source ($L_x = 3 \times 10^{37}$ ergs s^{-1}; $H_0 = 50$ km s^{-1} Mpc^{-1}) in a nearby galaxy, NGC 55. In an on-going collaborative effort with P. Szkody and her coworkers, who are carrying out optical spectroscopy and photometry of the objects, and V. Piirola and coworkers, who are carrying out polarimetry, J1047.1 + 6335 has been identified as a magnetic cataclysmic variable of $\simeq 19.4$ mag (K. P. Singh et al., ApJ, 453, L95 [1995]). J1802.1 + 1804 is a brighter ($\simeq 14.5$ mag) AM Her type binary (P. Szkody et al., ApJ, submitted [1996]). The variable X-ray source J1236.9 + 2656 seems to be a 17.5 mag quasar with narrow emission lines and redshift of ~ 0.2. J1757.8 + 0440 is most probably associated with the Bernard's star (Gliese 699) and was not identified earlier due to its high proper motion. J1219.7 + 3407, however, appears to have no optical counterpart down to the limiting magnitude (~ 21) in the digitized sky survey.